Endothelial antigen assembly leads to thrombotic complications in heparin-induced thrombocytopenia

Vincent Hayes,[1] Ian Johnston,[2] Gowthami M. Arepally,[3] Steven E. McKenzie,[4] Douglas B. Cines,[5] Lubica Rauova,[1,6] and Mortimer Poncz[1,6]

[1]Department of Pediatrics, Division of Hematology, The Children's Hospital of Philadelphia, Philadelphia, Pennsylvania, USA. [2]Department of Pharmacology, Perelman School of Medicine at the University of Pennsylvania, Philadelphia, Pennsylvania, USA. [3]Division of Hematology, Department of Medicine, Duke University School of Medicine, Durham, North Carolina, USA. [4]Thomas Jefferson University, Cardeza Foundation for Hematologic Research, Philadelphia, Pennsylvania, USA. [5]Department of Pathology and Laboratory Medicine and [6]Department of Pediatrics, Perelman School of Medicine at the University of Pennsylvania, Philadelphia, Pennsylvania, USA.

Heparin-induced thrombocytopenia (HIT) is a prothrombotic disorder initiated by antibodies against complexes between human platelet factor 4 (hPF4) and heparin. A better understanding of the events that initiate the prothrombotic state may improve approaches to antithrombotic management. Here, we visualized thrombus formation in an in vivo murine model and an endothelialized microfluidic system that simulate the pathogenesis of HIT. hPF4 released from platelets predominantly bound to peri-injury endothelium and formed HIT antigenic complexes that were dissociated by heparin. In mice expressing both hPF4$^+$ and human platelet IgG Fc receptor IIA (FcγRIIA), infusion of the HIT-like monoclonal antibody KKO increased fibrin and platelet deposition at sites of injury, followed immediately by antigen formation on proximate endothelial cells. After a few minutes, HIT antigen was detected within the thrombus itself at the interface between the platelet core and the surrounding shell. We observed similar results in the humanized, endothelialized microfluidic system. hPF4 and KKO selectively bound to photochemically injured endothelium at sites where surface glycocalyx was reduced. These studies support the concept that the perithrombus endothelium is the predominant site of HIT antigen assembly. This suggests that disrupting antigen formation along the endothelium or protecting the endothelium may provide a therapeutic opportunity to prevent thrombotic complications of HIT, while sparing systemic hemostatic pathways.

Introduction

Heparin-induced thrombocytopenia (HIT) is an iatrogenic disorder initiated by antibodies directed against a complex between a positively charged chemokine, platelet factor 4 (PF4, also known as CXCL4), and heparin (1) that can lead to limb- and life-threatening arterial or venous thrombi (2), which often occur at sites of vascular injury (3). HIT remains a common and serious disorder, even though the use of unfractionated heparin has been restricted to settings such as cardiopulmonary surgery (4, 5), where it remains the anticoagulant of choice (6). Present-day management with intense anticoagulation has not reduced the incidence of death or amputation, provides substantial but incomplete protection against recurrent thromboembolism, and is associated with a risk of bleeding for which antidotes are not available (7). A better understanding of the pathobiology of HIT might lead to novel disease-specific approaches that prevent immune complex–mediated thrombosis, with less reliance on intense systemic anticoagulation.

We have proposed a model to help explain the inordinate risk of thrombosis in patients with HIT compared with the thrombosis risk with other antibody-induced thrombocytopenias (8, 9): PF4 released from activated platelets binds to surface glycosaminoglycan side chains (GAGs) on intravascular and vascular cells. Infused heparin, which has a higher affinity for PF4 than for other GAGs, removes surface-bound PF4, forming circulating antigenic PF4-heparin complexes that fix complement and bind to CD21 on circulating antigen-presenting B cells (10). The antibodies that result bind to PF4-GAG complexes on the surface of platelets (9), monocytes (8), and neutrophils (11), leading to cell activation via Fc receptors (12), which promotes the generation of thrombin and other prothrombotic pathways (13).

Endothelial cells are targeted by HIT antibodies, at least in vitro (14–16), but the mechanism and in vivo relevance are unclear. The endothelium is covered by a complex surface layer termed the glycocalyx, which contains heparan sulfate–rich proteoglycans, glycoproteins, and associated plasma proteins (17, 18) that would be predicted to bind PF4 with greater affinity than the platelet surface. Binding of HIT antibody to cultured endothelial cells induces platelet adhesion and expression of tissue factor (15), but there is little direct evidence that HIT antibodies impair the natural antithrombotic properties of the endothelium in more biologically relevant models.

The spatial and temporal events that initiate thrombus development in HIT are not well delineated but are potentially of considerable import. Studies of platelet degranulation in the

Note regarding evaluation of this manuscript: Manuscripts authored by scientists associated with Duke University, The University of North Carolina at Chapel Hill, Duke-NUS, and the Sanford-Burnham Medical Research Institute are handled not by members of the editorial board but rather by the science editors, who consult with selected external editors and reviewers.

Conflict of interest: The authors have declared that no conflict of interest exists.

Submitted: September 28, 2016; **Accepted:** December 6, 2016.

Reference information: *J Clin Invest.* 2017;127(3):1090–1098.

https://doi.org/10.1172/JCI90958.

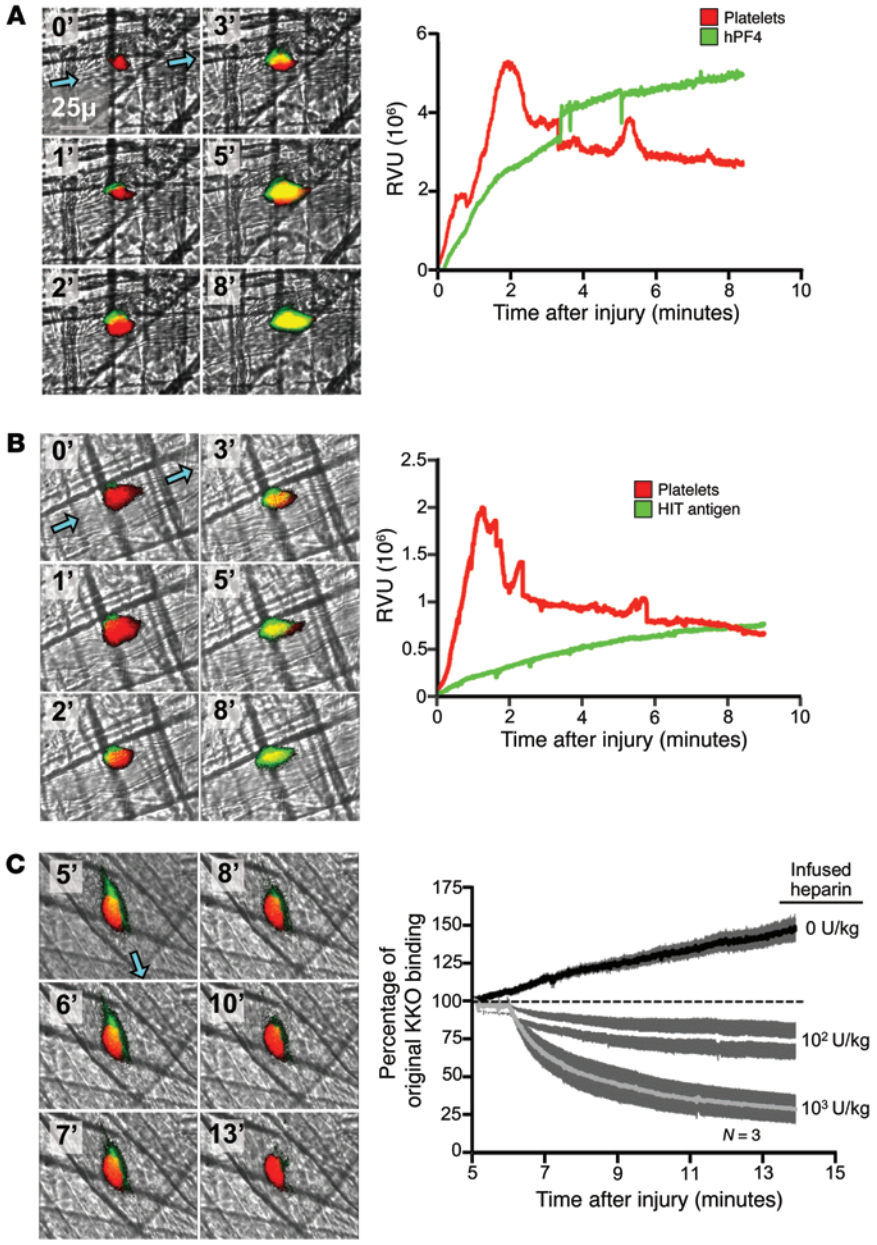

Figure 1. Widefield cremaster laser injury in a non-HIT hPF4⁺ murine model: In situ studies of hPF4 and HIT antigen distribution in thrombi. (**A**) Representative widefield study of more than 10 cremaster laser injuries in hPF4⁺ mice, with time 0 indicating the onset of injury. Images from a video of a laser injury; platelets are indicated in red, hPF4 is indicated in green, and the direction of blood flow in the vessel is denoted by blue arrows. Graph shows the accumulation of platelets and hPF4 over the study in relative value units (RVU) compared with time 0. (**B**) Same as in **A**, but with green showing binding of KKO to indicate the appearance of the HIT antigen. (**C**) Representative images from Supplemental Video 1 beginning 5 minutes after injury, the point at which 10^3 U/kg heparin was infused i.v. Platelets are indicated in red and KKO binding in green. The graph indicates that various doses of heparin were infused beginning 5 minutes after the cremaster injury. Percent mean ± 1 SEM for binding of KKO after heparin relative to the 5-minute time point is shown. The dashed line represents no change in KKO binding after heparin infusion compared with the 5-minute heparin time point. Original magnification, ×60.

cremaster arteriole laser injury model by our group and others (19–21) showed that the release of PF4 from platelets activated within a growing thrombus is likely to develop within the compacted core after a 2- to 3-minute delay and then expand outward (21). This would suggest that this high local concentration and sequestration of PF4 would lead to antigen formation on platelets within the core and the surrounding shell in preference to circulating leukocytes or endothelium and that HIT-associated antibodies must penetrate the core to propagate platelet-mediated thrombus extension. However, in HIT, we posit that antigen assembly occurs on multiple cell surfaces including monocytes, leukocytes, and endothelial cells. This difference is important, because one places the emphasis on interrupting platelet-platelet interactions, while the other suggests the value of therapies targeted to endothelial cells, among other cell types.

In this study, we used a previously described passive immunization model of HIT in mice double-transgenic for human PF4 and the human platelet IgG Fc receptor IIA (referred to hereafter as hPF4⁺/FcγRIIA⁺) (9, 22) and the cremaster arteriole laser injury model (23) to study in situ thrombus development in HIT. We extended these in vivo findings by using endothelialized microfluidic chambers, which allowed us to introduce localized hematoporphyrin-based photochemical injury to study the contribution of activated endothelium in a humanized system. Our data show that the perithrombus endothelium is the predominant site of HIT antigen formation, surprisingly at sites where the glycocalyx is depleted, followed by lower levels of antigen expression at the interface between the thrombus core and shell. We believe that these studies will serve to shift the focus of future studies on HIT pathogenesis and intervention to factors that regulate antigen assembly and the thrombotic consequences of antibody binding to the endothelium.

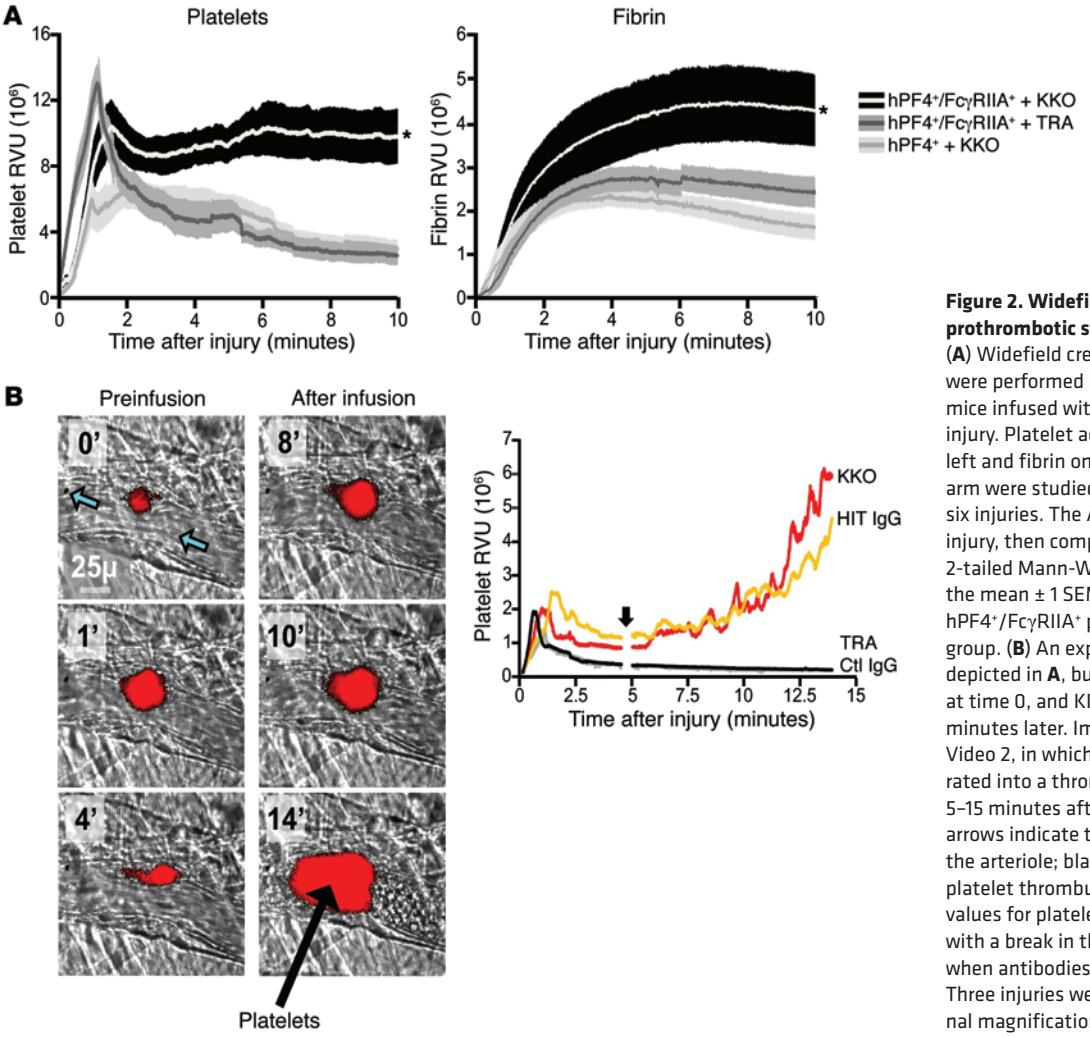

Figure 2. Widefield in situ studies of the prothrombotic state in a murine HIT model. (**A**) Widefield cremaster arteriole laser injuries were performed in hPF4⁺/FcγRIIA⁺ and hPF4⁺ mice infused with KKO or control TRA prior to injury. Platelet accumulation is shown on the left and fibrin on the right. Six mice from each arm were studied, and each mouse had five to six injuries. The AUC was calculated for each injury, then compared between groups by a 2-tailed Mann-Whitney *U* test. Data represent the mean ± 1 SEM. **P* < 0.05 comparing hPF4⁺/FcγRIIA⁺ plus KKO with either other group. (**B**) An experiment similar to the one depicted in **A**, but the injury was performed at time 0, and KKO (1 μg/g, i.v.) was infused 5 minutes later. Images are from Supplemental Video 2, in which platelets (red) were incorporated into a thrombus 0–4 minutes before or 5–15 minutes after the infusion of KKO. Blue arrows indicate the direction of blood flow in the arteriole; black arrow denotes the growing platelet thrombus. Graph shows the mean values for platelet incorporation into thrombi, with a break in the data just before 5 minutes, when antibodies were infused (vertical arrow). Three injuries were studied in each arm. Original magnification, ×60. Ctl, control.

Results

Distribution of HIT antigen after nonimmune vascular injury in hPF4⁺ mice. We previously proposed that a key step in the development HIT was the formation of antigen when positively charged hPF4 binds to negatively charged GAGs found on many cell surfaces (9). This model predicts that HIT antigen will form at all sites of vascular injury, even in the absence of HIT-associated antibodies. We tested this hypothesis in vivo using a cremaster arteriole laser injury model in hPF4⁺ mice. Following injury, hPF4, detected using a polyclonal anti-hPF4 antibody, and HIT antigen, detected using the HIT-like monoclonal antibody KKO (24), were present almost immediately on widefield microscopy, and the involved area expanded over the ensuing 3 minutes (Figure 1, A and B, respectively). This result demonstrates that hPF4 released as a result of thrombus formation accumulates locally in the form of PF4-containing complexes that can be recognized by HIT antibody in mice expressing hPF4 in their platelets with or without HIT.

We had reported that high doses of heparin attenuated the severity of thrombocytopenia in hPF4⁺/FcγRIIA⁺ mice (9). We postulated that this occurred because heparin can dissociate antigenic complexes from platelet surfaces at these concentrations (9), given its higher affinity for hPF4 than for surface GAGs (25). In turn, this generates the circulating hPF4-heparin complexes needed to induce an immune response. (25, 26) Therefore, we asked whether infusing unfractionated or low-molecular-weight heparin into hPF4⁺ mice would mobilize prebound PF4 and decrease retention of the HIT antigen at the site of thrombus formation. Binding of KKO to the site of thrombus formation decreased proportionally with the dose of either unfractionated heparin (Figure 1C and Supplemental Video 1; supplemental material available online with this article; https://doi.org/10.1172/JCI90958DS1) or low-molecular-weight heparin (Supplemental Figure 1) infused into hPF4⁺ mice. Importantly, however, even when mice were given 1,000 U/kg unfractionated heparin — a dose approximately 10-fold higher than therapeutic doses (27) — about 25% of the HIT antigen remained, suggesting that the vasculature continues to be a potential target for immune injury. Also of note, mice that did not receive heparin had the highest level of local HIT antigenicity, with an approximate 2-fold increase in HIT antigen compared with mice receiving a dose in the range normally given clinically (100 U/kg) (28).

Study of the prothrombotic state in a murine HIT model. We have previously shown that infusion of KKO or HIT-associated IgG (HIT-IgG) induces thrombocytopenia and a prothrombotic state in hPF4⁺/FcγRIIA⁺ mice (8, 9, 22). We recapitulated the prothrombotic state in the cremaster arteriole laser injury model. Injection of KKO into hPF4⁺/FcγRIIA⁺ mice enhanced platelet and fibrin

Table 1. Secondary growth of thrombi in hPF4⁺/FcγRIIA⁺ mice leading to an occluded vessel

	KKO (1 μg/g)	HIT IgG (50 μg/g)	TRA (1 μg/g)	Control IgG (50 μg/g)
No. of injuries	33	6	22	7
No. of occluded vessels	24	6	0	0
% of occluded vessels	72.7%[A]	100%[B]	0%	0%

Cremaster arterioles were injured by laser, and the accumulation of platelets was assessed. Five minutes later, KKO or TRA or HIT IgG or control IgG was infused i.v. at the indicated dose, and the site of injury was observed. The number of injured and occluded vessels with cessation of blood flow is indicated. [A]$P < 0.0001$, comparing the outcome after KKO versus TRA by 2-tailed Fisher's exact test. [B]$P < 0.001$, comparing the outcome after HIT IgG versus control IgG by 2-tailed Fisher's exact test.

accumulation in hPF4⁺/FcγRIIA⁺ mice, but not in hPF4⁺ mice or in hPF4⁺/FcγRIIA⁺ mice exposed to the isotype control antibody TRA (24) (Figure 2A).

Patients with HIT may be predisposed to develop thrombi at sites where vessels have been injured by catheters (3). To simulate this sequence in the cremaster model, we induced a thrombus in hPF4⁺/FcγRIIA⁺ mice, followed 5 minutes later by infusion of KKO or HIT-IgG. Preexisting thrombi expanded in mice given KKO or HIT-IgG, but not control antibodies (Figure 2B). These data also underestimate the severity of the prothrombotic state, because virtually all the vessels became occluded, limiting further thrombus expansion (Table 1 and Supplemental Video 2). Neither TRA nor normal IgG control infusions led to renewed growth of thrombi or vascular occlusion (Figure 2B and Table 1). Of note, thrombus regrowth began immediately after KKO was infused, but accelerated with time, demonstrating that a preexisting thrombus provides a potent nidus for expansion, leading to vascular occlusion in the setting of HIT antibodies.

Analysis of thrombus development in HIT by confocal microscopy. To begin to understand why thrombus regrowth was enhanced in HIT, we used confocal microscopy to examine the initial steps in thrombus formation following laser-induced arteriole injury in animals preinfused with KKO. Remarkably, the predominant site of KKO binding was the endothelium underlying and surrounding the thrombus, extending both upstream and downstream from the site of thrombosis (Figure 3A). The upstream binding appeared to be related to turbulent blood flow in this area (Supplemental Video 3). By 5 minutes after injury, KKO began to appear on platelets within the clot, which intensified over time at the boundary between the tightly packed core and surrounding looser shell of the thrombus (21) (enlarged image in Figure 3A and Figure 3B). We posit that this hemispheric zone of antigen was formed by the slow spread of α-granule release outward within the core until reaching the core-shell interface (21). Our studies suggest that more loosely bound platelets on the surface of the thrombus or caught in turbulent flow around the thrombus may make a more immediate and more significant contribution to the detectable PF4 in the thrombus. Moreover, the PF4 released from surface-bound platelets probably adheres better to the peri-injury endothelium, with its glycocalyx, which is rich in high-affinity heparan sulfate and dermatan sulfate (17), rather than to the thrombus platelets, with their lower affinity surface chondroitin sulfate (29, 30). This platelet-bound PF4 is likely swept downstream. The overlap of injured endothelium and KKO binding for annexin V is shown in Figure 3B and for factor Xa (FXa) in Supplemental Figure 2.

Infusion of KKO prior to laser injury in hPF4⁺/FcγRIIA⁺ mice further increased the size of the platelet-rich clot, and the total amount of HIT antigen in the perithrombus endothelium increased by approximately 3-fold compared with that detected in controls (Figure 3C). We observed similar increases in binding of annexin V and FXa to the perithrombus endothelium, suggesting that HIT antibodies exacerbated endothelial injury that could potentially cause a feed-forward cycle involving PF4-antigen formation, antibody binding, new injured endothelium, and spreading thrombosis.

Microfluidic studies of thrombosis in HIT. The in situ cremaster laser injury model enabled us to study the details of thrombus formation in vivo. However, the model is not fully humanized, and it is difficult to deduce the separate contributions from individual cellular components. To examine the role of the endothelium in HIT in a fully humanized context, we established endothelialized channels coated with HUVECs within a commercial microfluidic device (Figure 4A). Endothelial cells were grown to confluence, which was confirmed by the localization of platelet endothelial cell adhesion molecule 1 (PECAM-1) and expression of actin (Supplemental Figure 3A), and the cells were quiescent, given the absence of cell-surface P-selectin or release of von Willebrand factor (vWF) (Supplemental Figure 3B). The endothelium was injured by ROS made locally after exposure to light during the perfusion of human blood containing hematoporphyrin. In the studies below, injury was localized to an upstream portion of each channel (Supplemental Figure 4, A and B) without causing cell detachment (31), although the nuclei in the injured cells were pyknotic (Supplemental Figure 4B). Platelets adhered to the injured part of the channel, but not downstream (Figure 4B). Released PF4 was found surrounding platelet clumps and along the endothelium within the injured area. A decreasing gradient of PF4 binding to "uninjured" endothelium downstream of the injury was also in evidence (Figure 4, B–D). PF4 did not escape between injured endothelial cells to the abluminal surface (Figure 4D), a finding that was consistent with retention of cell-cell contact.

HIT was induced by adding KKO and hematoporphyrin to infused human whole blood prior to photochemical injury. KKO induced a significant increase in platelet adherence to HUVECs in the injured area compared with that observed with TRA (Figure 5A) and had a similar effect on similarly prepared adult human aortic endothelium (Supplemental Figure 5). Downstream of the injury, in the uninjured endothelium, no difference was noted between KKO and TRA exposure (Figure 5B). KKO also caused an increase of approximately 7-fold in PF4 binding to the injured endothelium compared with binding to the uninjured area, which was accompanied by an increase of approximately 16-fold in KKO binding to the injured endothelium compared with uninjured endothelium (Figure 5C). The injured endothelium showed an

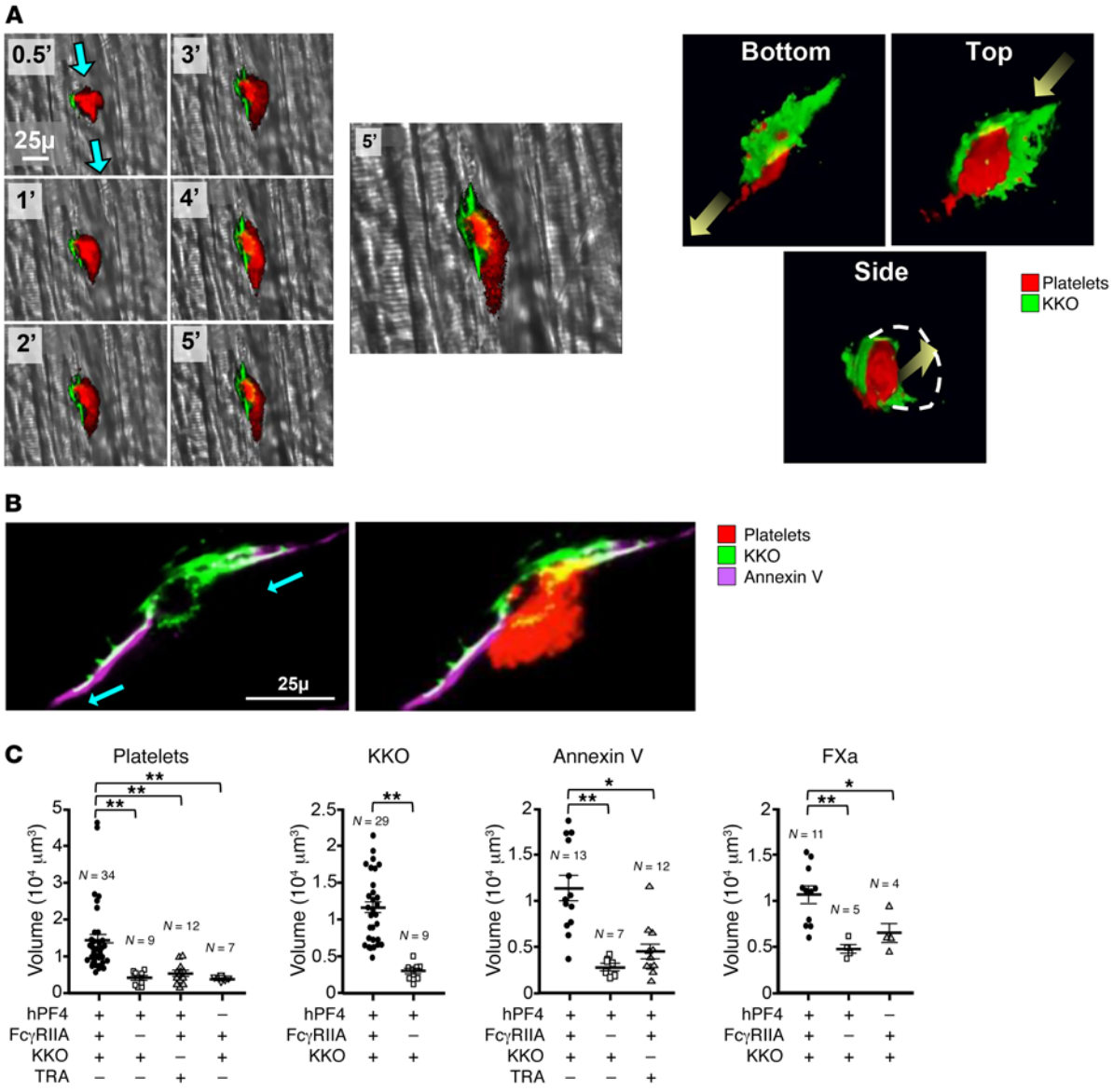

Figure 3. Confocal microscopic studies of a growing thrombus in HIT showing perithrombotic events. (**A**) Confocal microscopic images showing events in a representative cremaster arteriole injury in an hPF4$^+$/FcγRIIA$^+$ mouse infused with KKO. Platelets are shown in red. KKO binding is shown in green. Images on the left are from Supplemental Video 3 and include blue arrows showing the direction of blood flow. The image in the middle is an enlargement of the 5-minute time point, clearly showing a yellow semi-circle at the interface between the core and shell of the growing thrombus just becoming visible at 4 minutes. Images on the right show 3 different views of a 3D reconstruction of a thrombus, with the yellow arrow indicating the direction of blood flow. The dashed white circle indicates the outline of the vessel. (**B**) Confocal microscopic images, as in **A**, of another thrombus showing platelet accumulation (red) and binding of KKO (green) as well as staining with annexin V shown in purple as an indication of endothelial injury (50) and overlap with KKO binding shown in white. (**C**) Mice were preinfused with either KKO or TRA prior to creation of a thrombus. Binding of platelets, KKO, annexin V, and FXa to sites of vascular injury is shown. Data from the individual studies are shown as well as the mean ± 1 SEM (wide and narrow horizontal lines, respectively). The number of injuries studied for each parameter is indicated. *P < 0.001 and **P < 0.0001, by 2-way ANOVA. Original magnification, ×60.

increase of approximately 50-fold in P-selectin surface expression (P < 0.0001, Figure 5D) and release of vWF (Supplemental Figure 6) and a decrease of approximately 55% in glycocalyx staining by lectin compared with uninjured endothelium (P < 0.01, Figure 5D). Thus, the increase in binding of PF4 to the endothelium correlated with the loss of glycocalyx and its associated GAGs, as had been seen following other endothelial cell injuries (18, 32). Like the results obtained with infusion of KKO, infusion of HIT-associated IgG (300 μg/ml) along with whole blood led to occlusion of 6 of the 6 channels studied compared with 1 of 6 channels exposed to control IgG (P = 0.02, Table 1).

Discussion

HIT differs from other antibody-mediated thrombocytopenias by its propensity for significant thromboembolism (2, 33). We have attributed the prothrombotic state to the concurrent activation of multiple cell types by immune complexes. Platelets are dually activated by immune complexes through FcγRIIA (12) and by

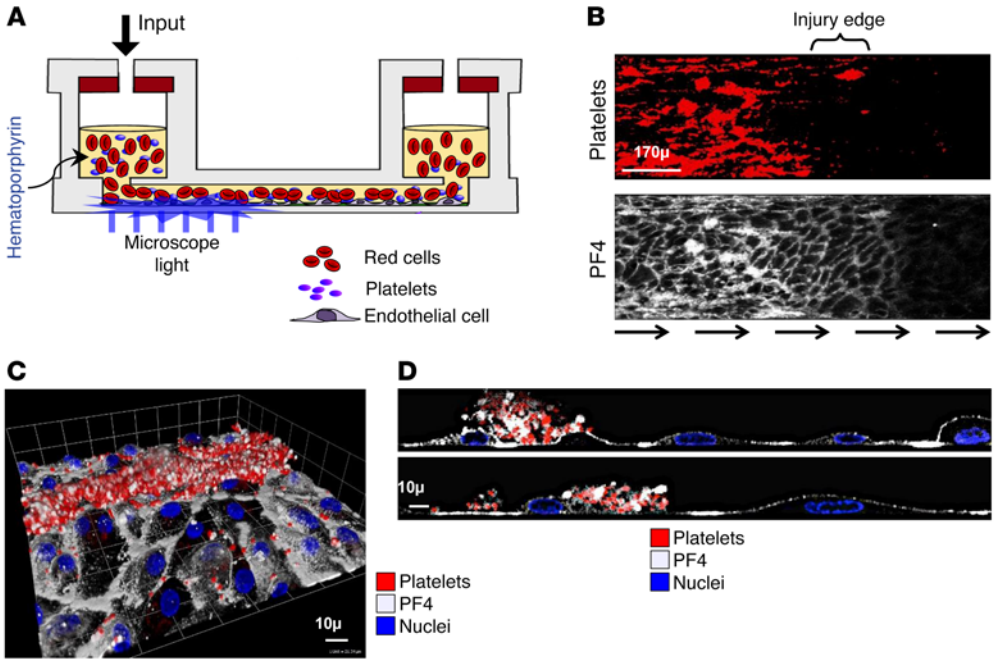

Figure 4. Endothelialized microfluidic channel studies after photochemical injury. (**A**) Schematic of microfluidic chamber with whole blood containing hematoporphyrin flowing into an endothelial cell–lined channel, with a light source to injure the endothelium. (**B**) Adhesion of platelets (red, top) and PF4 (white, bottom) at the junction between the injured and uninjured area from a representative study with infused blood, as in **A**. (**C** and **D**) Confocal images of the injured endothelium. (**C**) Top-down image of adherent platelets and released PF4 in the photochemically injured area. (**D**) Same image as in **C**, in a sagittal view. Original magnification, ×10 (**B**) and ×40 (**C** and **D**).

monocyte-generated thrombin (34). However, to date, the proposed involvement of the endothelium is based entirely on in vitro findings using cultured cells.

To better understand the prothrombotic nature of HIT, we performed video examination of thrombus formation in HIT both in vivo and in vitro. These in vivo cremaster studies involved laser-induced thrombi rather than spontaneous thrombi, but they allowed a detailed temporal analysis of events. We anticipate that the results of future similar studies of spontaneous thrombi in HIT mice would be consistent with our findings. Our in vivo studies showed that released PF4 was associated with formation of the HIT antigen, as identified using the monoclonal antibody KKO and by the binding of HIT-IgG on every thrombus. Infused heparin stripped this bound and antigenic PF4 away from the thrombus, decreasing surface antigenic complexes. These findings suggest that the pathogenic contribution of heparin to the development of HIT is solely the presentation of antigenic sites on PF4 to immunogenic cells and not exacerbation of the targeting of HIT antibodies onto thrombi. Indeed, stopping heparin may pose an increased risk of thrombosis that must be countered by instituting alternative anticoagulants (35).

Our in vivo findings also showed that soon after laser injury and thrombus formation, PF4 was localized predominantly on endothelial cells underlying and in the immediate vicinity of the clot. It is likely that endothelium-bound PF4 originated from transiently adherent platelets within the thrombus "shell" (21) or by platelets that had undergone activation within areas of turbulent blood flow. Only minutes later did PF4 begin to appear at the core-shell interface within the platelet-rich thrombus as a result of spreading degranulation, consistent with the appearance of surface P-selectin described by several groups (20, 21, 36) and perhaps due to less flow-induced dissociation within the core and transition zone within the shell of the clot (21). Our studies suggest that most α-granule proteins are released from outer layers or the exterior of the thrombus by transiently adherent platelets. Proteins that do not have a high affinity for surrounding cell surfaces are probably rapidly washed away, while those like PF4 may adhere to cells within or surrounding the thrombus.

The microfluidic photochemical injury studies, while involving a more diffuse vascular injury than did the cremaster injuries, support the conclusion that the endothelium is the predominant initial harbor for PF4 released from activated platelets and a target for HIT antibodies. While PF4 and KKO bind directly to platelets (9), monocytes (8), and neutrophils (37), we found that binding was more intense on injured endothelial cells. This is surprising, given that the glycocalyx is highly enriched for negatively charged side chains on its constituent proteoglycans, syndecans, and glypicans (17). These are candidate receptors for binding PF4, and one would have expected that with their loss, PF4 binding would have decreased. The loss of the glycocalyx involves multiple glycosidases or sheddases that remove hyaluronic acid residues and many other polyanions in this layer (38). We posit that the enhanced binding to injured glycocalyx may be due to the unveiling of a novel high-affinity binding site in the glycocalyx or the release of novel binding molecules from the injured endothelium that then reside in the remaining glycocalyx.

These studies support a pathogenic scenario, in which binding of PF4 leads to the formation of immune complexes on the endothelium, which may enhance platelet adhesion, enhance thrombin generation, and cause the release of additional PF4, which would sensitize the downstream endothelium and lead to a feed-forward pathway that propagates thrombosis. Such a phenomenon could contribute to the vessel occlusion we observed in the HIT cremaster arteriole model (Figure 2B) and, as observed earlier in HIT, to the presence of long, platelet-rich thrombi, resulting in the alternative name for this disorder of "white clot syndrome" (39). Whether these extended clots are related to a recruitment of undamaged endothelium in HIT needs to be examined. If this model is correct, it will be important to identify as potential therapeutic targets

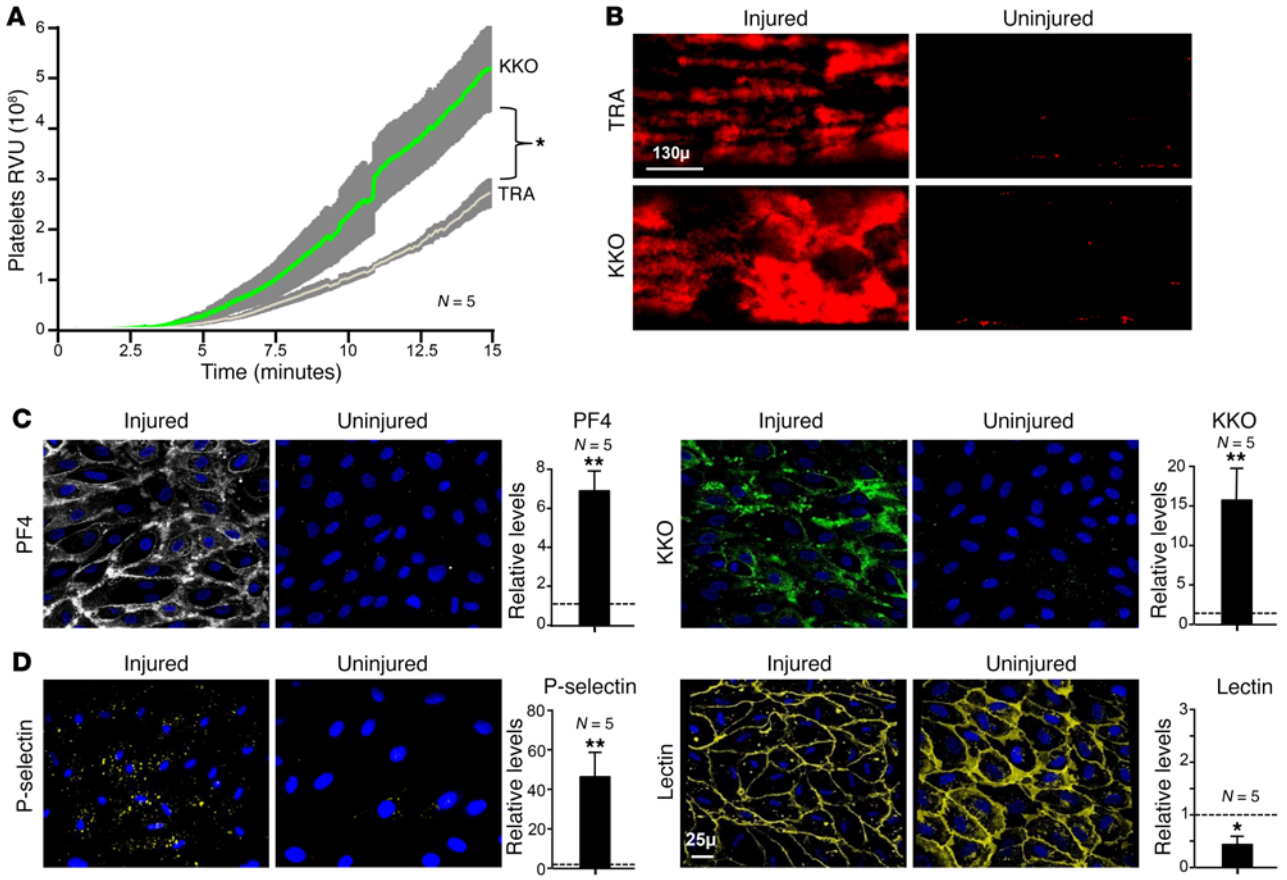

Figure 5. Studies of HIT in the endothelialized microfluidic channel photochemical injury system. (**A**) Platelet accumulation along HUVECs after photochemical injury perfused for 15 minutes with whole human blood containing either KKO or TRA. Data represent the mean ± 1 SEM. *$P < 0.0001$, for KKO versus TRA exposure by 2-tailed Student *t* test. (**B**) Images demonstrate platelets bound to representative fields of photochemically injured and uninjured areas of the channels shown in **A** from whole blood containing TRA or KKO. (**C**) Images of representative uninjured and injured areas and graphs of overall comparative measurements showing enhanced binding in injured versus uninjured areas of PF4 (white) and KKO binding (green) after infusion of whole blood, as in **A**. The mean relative binding for injured versus uninjured endothelium ± 1 SEM is shown. *$P < 0.01$ and **$P < 0.001$, by 2-sided Student's *t* test for injured versus uninjured areas, with an expectation of 1 and no change in binding (dashed line). (**D**) Same as in **C**, except for P-selectin staining (yellow) and lectin binding (yellow) in injured endothelium versus the downstream uninjured area. Lectin staining of the endothelium was decreased after injury. Original magnification, ×20.

the biophysical and biochemical changes in the endothelium that promote antigen and antibody binding. Moreover, these studies suggest that endothelial cell–targeted antiinflammatory and antithrombotic drugs (40, 41) might provide a rational intervention focused on the primary vortex of prothrombotic reactions that lead to thrombotic vascular occlusion.

Methods

Mice and human samples. Transgenic mice expressing platelet-specific hPF4 (42) (hPF4$^+$) and/or human FcγRIIA expressing its R^{131} isoform (43) (FcγRIIA$^+$) were studied. All transgenic mice were on a *Cxcl4*$^{-/-}$ background (44), as murine PF4 is not targeted by HIT-associated antibodies (24). This knockout setting, common to all the mice studied, is not specified hereafter. Genetic alterations were confirmed by the appropriate PCR analyses (42, 43). Mice were studied at 6 to 10 weeks of age. Only male mice were studied for the cremaster vessel injuries; however, we have not noted any prior sex difference in thrombosis in the passive immunization HIT murine model using a photochemical injury model (8).

Human blood (10–25 ml) from healthy volunteers for in vitro studies was drawn by gravity through a 19-gauge butterfly into sodium citrate (Sigma-Aldrich; 0.38% final concentration). Blood samples were stored at room temperature and used within 1 hour of being drawn. Deidentified plasma samples were obtained from patients who had a high pre-test probability of HIT on the basis of their clinical history (45), a positive PF4/heparin ELISA, and a positive serotonin release assay (46). For plasma samples from healthy donors, whole blood was centrifuged (200 *g*, 15 minutes), followed by centrifugation (2,000 *g*, 15 minutes) of the resultant platelet-rich plasma.

Heparins, antibodies, pooled IgGs, and other labeled probes. Unfractionated porcine heparin (BD) and low-molecular-weight heparin (enoxaparin; Novaplus) were used in this study. KKO, a mouse IgG $2b_K$ anti-hPF4/heparin monoclonal antibody, and TRA, a monoclonal IgG isotype control antibody (24), were purified from hybridoma supernatants. $F(ab')_2$ fragments of the monoclonal anti-mouse CD41 antibody MWReg30 (BD Biosciences) were used to detect murine platelets in the cremaster laser injury model. Anti–fibrin 59D8 monoclonal antibody was provided by Hartmut Weiler of the BloodCenter of Wiscon-

sin (Milwaukee, Wisconsin, USA) (47). Annexin V labeled with Alexa Fluor 647 was purchased from Thermo Fisher Scientific. Recombinant FXa labeled with Alexa Fluor 488 was provided by Rodney Camire of the Children's Hospital of Philadelphia. Mouse anti-human P-selectin antibody (clone CTB201) was purchased from Santa Cruz Biotechnology Inc. Polyclonal rabbit anti-human vWF antibody was purchased from Dako. hPF4 was visualized using polyclonal rabbit anti-hPF4 antibody (Abcam). All antibodies were either labeled using Alexa Fluor antibody–labeling kits according to the manufacturer's instructions or species-appropriate Alexa Fluor–conjugated secondary antibodies (all from Thermo Fisher Scientific). IgG was isolated from plasma from HIT patients and healthy donors using protein G agarose (Pierce, Thermo Fisher Scientific).

Cremaster laser injury studies. Intravital microscopy was performed as previously described (48). Vascular injury was induced with an SRS NL100 pulsed nitrogen dye laser (440 nm) focused on the vessel wall through the microscope objective. Arterioles of 20 to 40 μm diameter were selected, and the laser was pulsed until the vessels were perforated and a small number of red blood cells escaped. Antibodies and unfractionated porcine heparin (BD Biosciences) were infused as 100-μl boluses via a catheter placed into the jugular vein. Widefield and confocal microscopy were performed as described previously (20). Data were collected and widefield time-lapsed images of platelet and fibrin accumulation were analyzed using Slidebook 6.0 (Intelligent Imaging Innovations). Confocal *Z*-stacks were analyzed using Volocity 6.3 (PerkinElmer). hPF4$^+$, FcγRIIA$^+$, and hPF4$^+$/FcγRIIA$^+$ mice were studied. We studied 1–10 injuries per mouse during a maximum experimental time of 1 hour.

Endothelialized microfluidic studies. Microfluidic studies were performed using a BioFlux 200 Controller (Fluxion) with an attached heating stage set to 37°C as described previously (34). The BioFlux controller was used in conjunction with a Zeiss Axio Observer Z1 inverted microscope equipped with a motorized stage and an HXP-120 C metal halide illumination source. The microscope and acquisition were controlled using BioFlux Montage software with a MetaMorph-based platform (Molecular Devices). HUVECs and adult human aortic endothelial cells (both from Lonza), at passage 3–4 (5×10^6 cells), were seeded onto fibronectin-coated (50 μg/ml, Sigma-Aldrich) channels of 48-well BioFlux plates (Fluxion), allowed to adhere, then cultured at 37°C under 5% CO_2 in endothelial cell growth media (Lonza) until they reached confluency.

An HIT-like state was induced by adding KKO (10 μg/ml) to sodium citrate–anticoagulated whole blood from healthy donors immediately before infusion. Platelets in the whole blood were labeled by incubating the blood with 2 mM calcein AM (Thermo Fisher Scientific) for 20 minutes prior to infusion. To cause photochemical injury without disrupting the endothelial cell lining, hematoporphyrin (50 μg/ml final concentration; Sigma-Aldrich) was also added to the whole blood prior to infusion (31). Channels were exposed to blue light using the HXP-120 C light source with 475-nm excitation and 530-nm emission filters, allowing real-time, concurrent visualization of calcein AM–loaded platelets and ROS generation from hematoporphyrin. An exposure time of 50 ms at the highest intensity setting on the light source was used for all experiments. The blood was recalcified immediately before infusion with calcium chloride (11 mM final concentration). Infusion into endothelialized channels was done at a rate of 10 dynes/cm^2. Following injury, channels were washed with PBS and fixed with 2% paraformaldehyde (BD Biosciences) for confocal studies of P-selectin, PF4, and KKO. To measure the glycocalyx thickness, HUVECs lining the channels were stained with 1 μg/ml DyLight 488–labeled *Lycospersicon esculentum* lectin (Vector Laboratories) for 20 minutes prior to fixation (49). Endothelial cell nuclei were identified by staining with 5 μg/ml Hoescht 33342 (Thermo Fisher Scientific) for 20 minutes. Stained channels were imaged with a Zeiss LSM 710 laser scanning confocal microscope. Data were analyzed using Slidebook 6.0 (Intelligent Imaging Innovations) for photochemical injuries or Volocity 6.3 (PerkinElmer) for confocal images acquired after fixation.

Statistics. Differences between 2 groups were compared using a 2-sided Student's *t* test or a Mann-Whitney *U* test. Differences between more than 2 groups were determined by 2-way ANOVA with Sidak's correction for multiple comparisons. Occlusion studies were compared using a 2-sided Fisher's exact test. Statistical analyses were performed using Microsoft Excel 2011 and GraphPad Prism 6.0 (GraphPad Software). Differences were considered significant when *P* values were less than or equal to 0.05.

Study approval. All animal procedures were approved by the IACUC of the Children's Hospital of Philadelphia and in accordance with NIH guidelines (*Guide for the Care and Use of Laboratory Animals*. National Academies Press. 2011.) and the Animal Welfare Act. Human blood was collected after signed, informed consent was provided by healthy donors, and approval for studies using human blood was obtained from the Children's Hospital of Philadelphia Institutional Human Review Board in accordance with Declaration of Helsinki principles.

Author contributions

VH designed and performed most of the experiments, was primary author of the manuscript, and prepared the first draft of the manuscript. IJ performed microfluidic studies and helped write the related sections of the manuscript. GMA and SEMcK provided important insights into the proposed studies and outcomes interpretation. DBC and LR helped with study design, data analysis, and editing of the manuscript. MP provided overall scientific guidance and helped prepare the manuscript.

Acknowledgments

This work was supported by funding from the NIH (P01 HL110860, to GMA, SEMcK, DBC, LR, and MP).

Address correspondence to: Mortimer Poncz, Children's Hospital of Philadelphia, 3615 Civic Center Boulevard, 317 ARC, Philadelphia, Pennsylvania 19104, USA. Phone: 215.590.3574; E-mail: poncz@email.chop.edu.

1. Amiral J, et al. Platelet factor 4 complexed to heparin is the target for antibodies generated in heparin-induced thrombocytopenia. *Thromb Haemost*. 1992;68(1):95–96.
2. Greinacher A, Farner B, Kroll H, Kohlmann T, Warkentin TE, Eichler P. Clinical features of heparin-induced thrombocytopenia including risk factors for thrombosis. A retrospective analysis of 408 patients. *Thromb Haemost*. 2005;94(1):132–135.
3. Hong AP, Cook DJ, Sigouin CS, Warkentin TE. Central venous catheters and upper-extremity deep-vein thrombosis complicating immune heparin-induced thrombocytopenia. *Blood*. 2003;101(8):3049–3051.

4. Martel N, Lee J, Wells PS. Risk for heparin-induced thrombocytopenia with unfractionated and low-molecular-weight heparin thromboprophylaxis: a meta-analysis. *Blood*. 2005;106(8):2710–2715.
5. Linkins LA. End of the road for heparin thromboprophylaxis. *Blood*. 2016;127 (16):1945–1946.
6. Riess FC. Anticoagulation management and cardiac surgery in patients with heparin-induced thrombocytopenia. *Semin Thorac Cardiovasc Surg*. 2005;17(1):85–96.
7. Kelton JG, Hursting MJ, Heddle N, Lewis BE. Predictors of clinical outcome in patients with heparin-induced thrombocytopenia treated with direct thrombin inhibition. *Blood Coagul Fibrinolysis*. 2008;19(6):471–475.
8. Rauova L, et al. Monocyte-bound PF4 in the pathogenesis of heparin-induced thrombocytopenia. *Blood*. 2010;116 (23):5021–5031.
9. Rauova L, Zhai L, Kowalska MA, Arepally GM, Cines DB, Poncz M. Role of platelet surface PF4 antigenic complexes in heparin-induced thrombocytopenia pathogenesis: diagnostic and therapeutic implications. *Blood*. 2006;107(6):2346–2353.
10. Khandelwal S, et al. The antigenic complex in HIT binds to B-cells via complement complement receptor 2 (CD21). *Blood*. 2016;128(14):1789–1799.
11. Petersen F, Brandt E, Lindahl U, Spillmann D. Characterization of a neutrophil cell surface glycosaminoglycan that mediates binding of platelet factor 4. *J Biol Chem*. 1999;274 (18):12376–12382.
12. Kelton JG, et al. Heparin-induced thrombocytopenia: laboratory studies. *Blood*. 1988;72(3):925–930.
13. Warkentin TE, et al. Sera from patients with heparin-induced thrombocytopenia generate platelet-derived microparticles with procoagulant activity: an explanation for the thrombotic complications of heparin-induced thrombocytopenia. *Blood*. 1994;84(11):3691–3699.
14. Blank M, et al. Anti-platelet factor 4/heparin antibodies from patients with heparin-induced thrombocytopenia provoke direct activation of microvascular endothelial cells. *Int Immunol*. 2002;14(2):121–129.
15. Cines DB, Tomaski A, Tannenbaum S. Immune endothelial-cell injury in heparin-associated thrombocytopenia. *N Engl J Med*. 1987;316(10):581–589.
16. Visentin GP, Ford SE, Scott JP, Aster RH. Antibodies from patients with heparin-induced thrombocytopenia/thrombosis are specific for platelet factor 4 complexed with heparin or bound to endothelial cells. *J Clin Invest*. 1994;93(1):81–88.
17. Marki A, Esko JD, Pries AR, Ley K. Role of the endothelial surface layer in neutrophil recruitment. *J Leukoc Biol*. 2015;98(4):503–515.
18. Reitsma S, Slaaf DW, Vink H, van Zandvoort MA, oude Egbrink MG. The endothelial glycocalyx: composition, functions, and visualization. *Pflugers Arch*. 2007;454(3):345–359.
19. Falati S, et al. Accumulation of tissue factor into developing thrombi in vivo is dependent upon microparticle P-selectin glycoprotein ligand 1 and platelet P-selectin. *J Exp Med*. 2003;197(11):1585–1598.
20. Neyman M, Gewirtz J, Poncz M. Analysis of the spatial and temporal characteristics of platelet-delivered factor VIII-based clots. *Blood*. 2008;112(4):1101–1108.
21. Stalker TJ, et al. Hierarchical organization in the hemostatic response and its relationship to the platelet-signaling network. *Blood*. 2013;121(10):1875–1885.
22. Reilly MP, et al. Heparin-induced thrombocytopenia/thrombosis in a transgenic mouse model requires human platelet factor 4 and platelet activation through FcgammaRIIA. *Blood*. 2001;98(8):2442–2447.
23. Falati S, Gross P, Merrill-Skoloff G, Furie BC, Furie B. Real-time in vivo imaging of platelets, tissue factor and fibrin during arterial thrombus formation in the mouse. *Nat Med*. 2002;8(10):1175–1181.
24. Arepally GM, et al. Characterization of a murine monoclonal antibody that mimics heparin-induced thrombocytopenia antibodies. *Blood*. 2000;95(5):1533–1540.
25. Suvarna S, et al. Determinants of PF4/heparin immunogenicity. *Blood*. 2007;110(13):4253–4260.
26. Suvarna S, Qi R, Arepally GM. Optimization of a murine immunization model for study of PF4/heparin antibodies. *J Thromb Haemost*. 2009;7(5):857–864.
27. Hirsh J, Anand SS, Halperin JL, Fuster V, American Heart Association. AHA Scientific Statement: Guide to anticoagulant therapy: heparin: a statement for healthcare professionals from the American Heart Association. *Arterioscler Thromb Vasc Biol*. 2001;21(7):E9–E9.
28. Soleimannejad M, et al. Activated clotting time level with weight based heparin dosing during percutaneous coronary intervention and its determinant factors. *J Cardiovasc Thorac Res*. 2014;6(2):97–100.
29. Nader HB. Characterization of a heparan sulfate and a peculiar chondroitin 4-sulfate proteoglycan from platelets. Inhibition of the aggregation process by platelet chondroitin sulfate proteoglycan. *J Biol Chem*. 1991;266(16):10518–10523.
30. Ward JV, Packham MA. Characterization of the sulfated glycosaminoglycan on the surface and in the storage granules of rabbit platelets. *Biochim Biophys Acta*. 1979;583(2):196–207.
31. Nishimura S, et al. In vivo imaging visualizes discoid platelet aggregations without endothelium disruption and implicates contribution of inflammatory cytokine and integrin signaling. *Blood*. 2012;119(8):e45–e56.
32. Ushiyama A, Kataoka H, Iijima T. Glycocalyx and its involvement in clinical pathophysiologies. *J Intensive Care*. 2016;4(1):59.
33. Warkentin TE, et al. Heparin-induced thrombocytopenia in medical surgical critical illness. *Chest*. 2013;144(3):848–858.
34. Tutwiler V, et al. Platelet transactivation by monocytes promotes thrombosis in heparin-induced thrombocytopenia. *Blood*. 2016;127(4):464–472.
35. Warkentin TE, Greinacher A. Heparin-induced thrombocytopenia: recognition, treatment, and prevention: the Seventh ACCP Conference on Antithrombotic and Thrombolytic Therapy. *Chest*. 2004;126(3 Suppl):311S–337S.
36. Gross PL, Furie BC, Merrill-Skoloff G, Chou J, Furie B. Leukocyte-versus microparticle-mediated tissue factor transfer during arteriolar thrombus development. *J Leukoc Biol*. 2005;78(6):1318–1326.
37. Xiao Z, Visentin GP, Dayananda KM, Neelamegham S. Immune complexes formed following the binding of anti-platelet factor 4 (CXCL4) antibodies to CXCL4 stimulate human neutrophil activation and cell adhesion. *Blood*. 2008;112(4):1091–1100.
38. Becker BF, Jacob M, Leipert S, Salmon AH, Chappell D. Degradation of the endothelial glycocalyx in clinical settings: searching for the sheddases. *Br J Clin Pharmacol*. 2015;80(3):389–402.
39. Daubert GP. The white clot syndrome. *J Clin Pharm Ther*. 2005;30(6):503.
40. Aisiku O, et al. Parmodulins inhibit thrombus formation without inducing endothelial injury caused by vorapaxar. *Blood*. 2015;125(12):1976–1985.
41. Greineder CF, et al. Molecular engineering of high affinity single-chain antibody fragment for endothelial targeting of proteins and nanocarriers in rodents and humans. *J Control Release*. 2016;226:229–237.
42. Zhang C, et al. Localization of distal regulatory domains in the megakaryocyte-specific platelet basic protein/platelet factor 4 gene locus. *Blood*. 2001;98(3):610–617.
43. McKenzie SE, et al. The role of the human Fc receptor Fc gamma RIIA in the immune clearance of platelets: a transgenic mouse model. *J Immunol*. 1999;162(7):4311–4318.
44. Eslin DE, et al. Transgenic mice studies demonstrate a role for platelet factor 4 in thrombosis: dissociation between anticoagulant and antithrombotic effect of heparin. *Blood*. 2004;104(10):3173–3180.
45. Cuker A, et al. The HIT Expert Probability (HEP) Score: a novel pre-test probability model for heparin-induced thrombocytopenia based on broad expert opinion. *J Thromb Haemost*. 2010;8(12):2642–2650.
46. Sheridan D, Carter C, Kelton JG. A diagnostic test for heparin-induced thrombocytopenia. *Blood*. 1986;67(1):27–30.
47. Hui KY, Haber E, Matsueda GR. Monoclonal antibodies to a synthetic fibrin-like peptide bind to human fibrin but not fibrinogen. *Science*. 1983;222(4628):1129–1132.
48. Celi A, et al. Thrombus formation: direct real-time observation and digital analysis of thrombus assembly in a living mouse by confocal and wide-field intravital microscopy. *J Thromb Haemost*. 2003;1 (1):60–68.
49. Barkefors I, Aidun CK, Ulrika Egertsdotter EM. Effect of fluid shear stress on endocytosis of heparan sulfate and low-density lipoproteins. *J Biomed Biotechnol*. 2007;2007:65136.
50. Ivanciu L, Krishnaswamy S, Camire RM. New insights into the spatiotemporal localization of prothrombinase in vivo. *Blood*. 2014;124(11):1705–1714.